Experimental investigation of a two-truck platoon considering inter-vehicle distance, lateral offset and yaw

Journal of Wind Engineering & Industrial Aerodynamics 213 (2021) 104596

Contents lists available at ScienceDirect

Journal of Wind Engineering & Industrial Aerodynamics

journal homepage: www.elsevier.com/locate/jweia

Experimental investigation of a two-truck platoon considering inter-vehicle distance, lateral offset and yaw

Johannes Törnell [a,*], Simone Sebben [a], Per Elofsson [b]

[a] Department of Mechanics and Maritime Science, Chalmers University of Technology, SE-412 96, Gothenburg, Sweden
[b] Fluid Mechanics, Scania CV, SE-151 87, Södertälje, Sweden

ARTICLE INFO

Keywords:
truck
Platooning
Drag
Wind tunnel experiments
Lateral offset
Close-proximity
Reynolds independence
Inter-vehicle distance

ABSTRACT

In recent years a renewed interest in platooning has emerged due to increasing pressure on vehicle manufacturers to reduce greenhouse gas emissions of their fleets. Vehicles traveling in close proximity have been studied in some depth, particularly simplified bodies and North American trucks. Still, there is a lack of understanding of the benefits of platooning for European style trucks. In this study, experiments were undertaken using two 1:6 scale detailed cab over engine tractor-trailer models in a wind tunnel with a moving ground. Surface pressures were measured on both trucks, while force measurements were taken on the model placed on the belt. Inter-vehicle distance, lateral offset, and yaw conditions were varied. Results show that a reduction of drag for the platoon is seen as the inter-vehicle distance decreases. For the leading truck, the reduction is due to an increased base pressure caused by the truck behind. The trailing truck has a more complex behavior and is sensitive to yaw changes. At short inter-vehicle distances, the leading truck loses in performance with a lateral offset, while the trailing truck gains in performance if under yaw conditions. To aid the flow analysis, numerical simulations were undertaken for some conditions studied experimentally.

1. Introduction

A renewed interest in the concept of platooning has emerged in recent years with new stricter requirements on vehicle greenhouse gas emissions and further improvements in vehicle automation and sensor technology. Platooning is used in this paper to describe vehicles driving in close proximity, which reduces aerodynamic drag. In addition to road vehicles, the concept has been applied to sports, such as cycling and motorsports, Blocken et al. (2018a); Jacuzzi and Granlund (2019); Blocken et al. (2018b), as well as trains, where the spacing between containers has been studied for optimal drag by, for example, Li et al. (2017); Maleki et al. (2019). Additionally, the flow phenomena in platooning can be connected to those occurring in the tractor-trailer gap of single trucks, Allan (1981); Östh and Krajnovic (2012).

A significant body of research has been carried out with regard to the fuel consumption and aerodynamic drag of trucks traveling in close proximity; however, most of these have been done with small scale models in the aerodynamic drag studies and on North American style tractor-trailer combinations. All of the currently published experimental studies have used a stationary floor and non-rotating wheels and were performed at low Reynolds numbers. In the studies performed on North American trucks, Salari and Ortega (2018); Lammert et al. (2017); McAuliffe and Ahmadi-Baloutaki (2018, McAuliffe and Ahmadi-Baloutaki, 2019, both the effects of inter-vehicle distance (IVD), lateral offset, yaw, and interference of varied vehicle types were investigated. All studies have shown that there is a continuous decrease of drag with reduced IVD for the leading vehicle and a general decrease in drag of the trailing vehicle, but with an increase occurring at roughly 3m–20m. McAuliffe and Ahmadi-Baloutaki, 2019 argued that when considering the benefits of platooning, these have to be compared to drag values that are representative for a vehicle driving in realistic road conditions, that is considering traffic. McAuliffe and Ahmadi-Baloutaki (2018) also observed that the engine cooling flow decreases by up to 70% at very short distances which is a potential negative effect of platooning.

Studies utilizing simplified models, i.e., Hammache et al. (2002); Schito and Braghin (2012); Le Good et al. (2018, 2019); Tsuei and Ömer Savaş (2001); Fletcher and Stewart (1986); Watkins and Vino (2008), have found that the most beneficial combinations are those where the non-streamlined ends are facing each other, for example, a square back in front of a flat front. Further, the studies show that the changes to drag of North American style trucks were similar to those of simple, more square models. There were, however, cases where no benefit was seen with a

* Corresponding author.
E-mail addresses: Johannes.Tornell@chalmers.se (J. Törnell), Simone.Sebben@chalmers.se (S. Sebben), Per.Elofsson@scania.com (P. Elofsson).

https://doi.org/10.1016/j.jweia.2021.104596
Received 6 October 2020; Received in revised form 4 March 2021; Accepted 6 March 2021
Available online 13 April 2021

Abbreviation

IVD	Inter-vehicle distance
COE	Cab over engine
C_p	Coefficient of Pressure
C_D	Coefficient of Drag

platooning scenario. This tended to be when an aerodynamic base of the leading vehicle was combined with a smooth and aerodynamic front of the trailing vehicle. Similar results have been observed in studies of platoons of passenger cars, however, with low sensitivity to yaw when this has been investigated, Marcu and Browand (1999); Hong et al. (1998); Ebrahim and Dominy (2020).

It is clear from the literature that there is a gap in knowledge, both in the behavior of European, cab over engine (COE) style trucks, but also of the aerodynamic performance in more realistic settings with detailed models, ground simulation, and high Reynolds numbers. The influence on drag of ground simulation and rotating wheels has long been known in aerodynamics, especially for passenger vehicles, as discussed in Howell and Everitt (1981); Hackett et al. (1987); Yamashita et al. (2018). However, for heavy vehicles, according to Söderblom et al.; Söderblom (2012), their influence is smaller and more local, with changes appearing around the wheel wake region and in the lower part of the base wake, with some upwash being created near the centerline. In their study, these local changes had no impact on the rest of the rear wake, nor on drag. Still, the presence of a ground simulation system has shown to be of significance for the Reynolds behavior, Baker and Brockie (1991); Burgin et al. (1986); Sardou (1986). The present study provides experimental data from highly detailed COE models obtained in a wind tunnel fitted with a moving ground under flow conditions shown to be in the Reynolds number independent range. Furthermore, it provides useful insight on the drag behavior of the system and on the areas of the truck which are affected when inter-vehicle distance (IVD), lateral offset, and yaw angle are varied. As the experimental facility used had limited possibilities of performing measurements on the flow, Computational Fluid Dynamics (CFD) simulations were conducted as an addition to the analysis.

2. Method

This section describes the wind tunnel facilities, the models, the experimental setup, and the CFD methodology used to complement the analysis of the results.

2.1. Wind tunnel

The facility used in this study was the Volvo Cars Aerodynamic wind tunnel. It is a slotted wall wind tunnel with a slot open area ratio of 30% and a cross-sectional area of 27.1m^2, yielding a blockage of 1.07% for a single truck model at zero yaw. The tunnel is also equipped with a ground simulation and a boundary layer control system. The boundary layer control system consists of a scoop suction, distributed suction as well as tangential blowing behind each of the five belts of the ground simulation system. The distributed suction, through more than 100 000 holes perforated in the floor, prevents a boundary layer build-up, and is split into two parts. The first part, between the scoop and the turntable, consists of a perforated floor with an open area ratio of 8.9%. The second part, with an open area ratio of 4.5%, is mounted on the turntable together with the moving belts and the tangential blowers. The five-belt system consists of four wheel drive units and a center belt. The center belt is 5.3m long and 1m wide and is approximately twice as long and wide as the truck model (see model dimensions on the next section). The forces are measured through an underfloor balance and the repeatability of the measurements is roughly 0.5% of a single isolated truck drag. The forces are averaged over 20s, as this is the standard procedure in the wind tunnel. As a higher velocity and smaller scale than normal is used in this study, this should be sufficient. An outline of the wind tunnel test section and the ground simulations system is shown in Fig. 1, where the light green area is the space which was occupied by vehicles during the test while varying inter-vehicle distance (IVD), lateral offset and yaw. The red filled rectangle represents the model that was attached to the balance and the two outlined blanked rectangles exemplify the model moved around to create the platoon. Considering these limitations, a maximum of 30m IVD and 5-degree yaw angle were investigated. This yaw value is commonly used in truck development as the drag coefficient measured at 5° is a good approximation of a wind averaged drag for a COE tractor-trailer combination. Normally, the deviation between the 5-degree yaw drag value and the wind averaged drag value, as defined in J1252 (Rev. August 2012), is about 1% for this vehicle combination.

For more information on the wind tunnel, its ground simulation system, and flow quality, see Sternéus et al. (2007) and Ljungskog (2019).

2.2. Test objects

The models used in this study, seen in Fig. 2, were a slightly simplified 1/6th scale cab over engine (COE) tractor combined with a three-axle semi-trailer. Both tractors were equipped with rolling wheels, however, only one model had a coating on the wheels and could be driven by the center belt. This model, termed as the measurement model, was kept fixed during the tests. This was the only possible alternative considering the number of configurations planned, the tunnel availability for this campaign and the long time necessary to place the measurement model safely in position on the belt (approximately 8 h). The second model, with stationary wheels, is referred to as the dummy model and was moved around to change both IVD and lateral offset. The tractors of each vehicle had fairly detailed engine bays where the engine and gearbox were simplified to only the larger parts with no cabling, see Fig. 2b. The cooling package consisted of a mesh and a honeycomb setup.

The measurement model had a trailer equipped with a detailed undercarriage as shown in Fig. 2c, while the trailer of the dummy model had a slightly simplified undercarriage, which consisted of a box with added half disks as wheels and skirts. Although the differences in the undercarriage and the non-rotating wheel condition of the dummy model could cause local variations in the flow close to the ground and affect the drag of the vehicle, these were not possible to quantify and assumed not to have any major impact on the results of the platoon as a system. In this study, the function of the dummy model was to create a blockage effect, and thereby change the pressures in front or behind the measurement model, rather than to guarantee the same drag and flow structures. Additionally, it is reasonable to expect that in real situations, vehicles traveling in a platoon will not be exactly alike, and that the main aerodynamic gains will come from the models being in close proximity, rather than from specific details of the undercarriages.

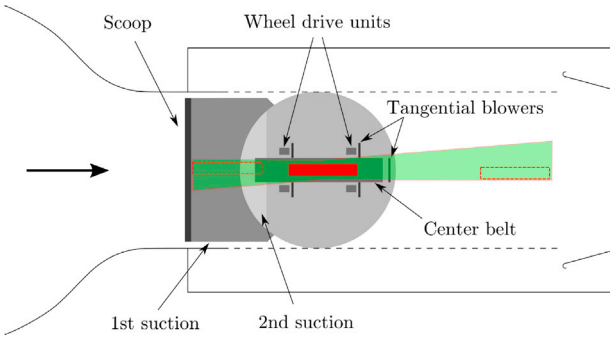

Fig. 1. Layout of the ground simulation system and the available space in the test section for varying IVD, lateral offset, and yaw.

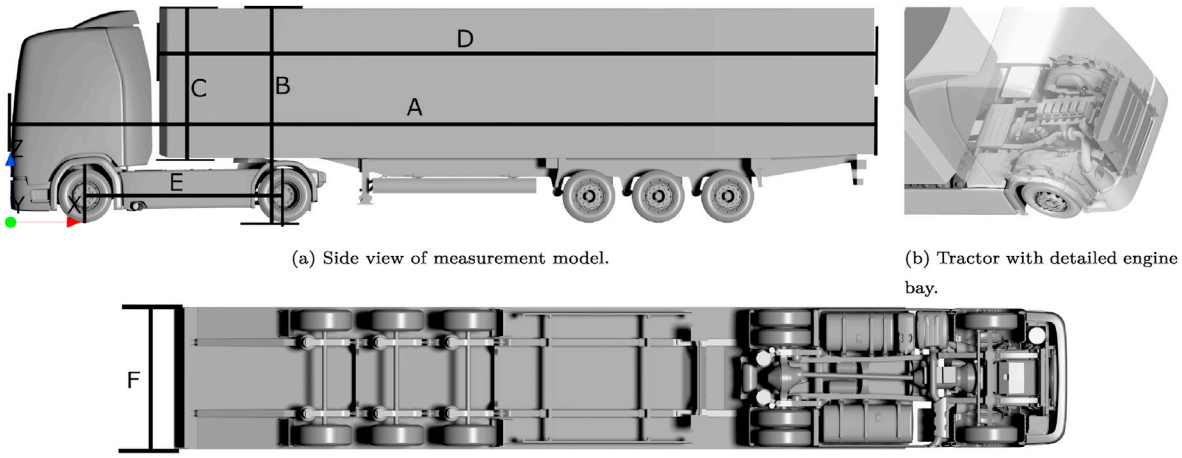

(a) Side view of measurement model.

(b) Tractor with detailed engine bay.

(c) Undercarriage of the measurement model, the dummy model tractor is identical.

Fig. 2. Models used in this study and relevant dimensions. A = 2.720m, B = 667 mm, C = 0.467m, D = 2.250, E = 0.625m, F = 0.433m.

The measurement model was instrumented with time-resolving pressure sensors while the dummy model had mean pressure sensors. Fig. 3 shows the location of the pressure taps, and the colors represent the different surfaces for mean pressures. As the front corners are very sensitive to separation, it was decided not to add pressure taps on them. The pressure was, however, measured on the sides and roof, just behind the radii, but are used here to infer the pressure trends on the radii. Additionally, the taps were placed above the height of local influences of the flow from the undercarriage and the wheel rotation.

The models have a frontal area of 0.28 m^2.

2.3. Experimental setup

The models required a customized mounting solution and experienced personnel to guarantee proper safety when placed on the moving belt. As the measurement model and center belt were not strong enough to support the full weight of the model, it had to be suspended from the roof of the wind tunnel. This was done by fastening two 6 mm steel cables to a beam in the ceiling of the slotted wall test section. To constrain the truck in the ground plane, four 6 mm steel cables were attached from the trailer of the model to the restraint posts of the wind tunnel which are usually attached to the floor of the vehicle being tested, see Fig. 4. These posts are connected to the balance allowing for the forces to be measured on the model. The holding cables have a frontal area of roughly $0.025m^2$, with most of the area coming from the two attaching the model to the ceiling. It is expected that about half of the drag force exerted on them is experienced by the balance. Although the cables will have some impact on the absolute values measured on the model, their effect is likely to be small and will be here neglected. Additionally, as the present work focuses on drag delta trends, these should not be influenced by the presence of the cables, as they are mostly outside the area which will be affected by the vehicle in front or behind. Furthermore, the rolling resistance of the wheels was removed by spinning up the center-belt to the correct speed with the wind off and the balance was then tared. This should remain accurate even if the model moves slightly due to lift forces as the wheels are floating and only attached to the truck via a pivot.

The dummy model was attached to the floor of the wind tunnel by 6 mm cables to existing mounting holes and when placed above the center-belt, it was supported under the wheels by a 20 mm thick beveled beam to avoid damage to the center belt. This slight change in height of the dummy model could potentially have a small effect on the results, but is here neglected as there was no other possible way to mount it.

For all configurations, all five belts were run at the corresponding wind speed to minimize the force on the wheel-drive units, as these were attached to the balance. The boundary layer control system was run in two different modes based on if the dummy model was in front of or behind the measurement model. When the dummy model was behind the measurement model, the suction scoop and distributed suction system were turned on, when the dummy model was in front of the measurement model, the distributed suction system was turned off as the dummy model was placed on top of the distributed suction system itself. The tangential blowing system was turned off for all tests to simplify future comparisons with numerical simulations. Fig. 5 shows the different position parameters that were varied during the experiment. As can be seen,

(a) Front of the truck, the colors represent the different areas of

(b) Base of the truck.

Fig. 3. Pressure tap locations.

Fig. 4. Mounting solution. Here, the leading truck is the dummy model, and the trailing truck is the measurement model.

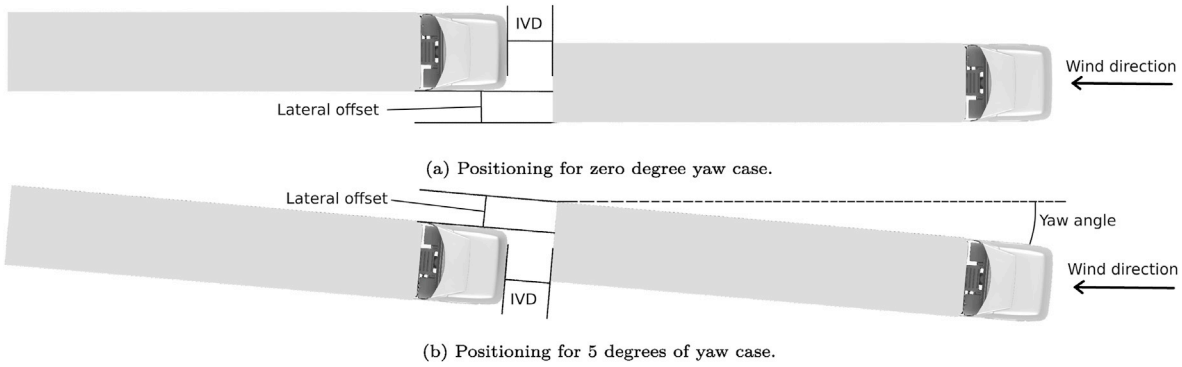

(a) Positioning for zero degree yaw case.

(b) Positioning for 5 degrees of yaw case.

Fig. 5. Definitions of the three position components, inter-vehicle distance, lateral offset, and yaw angle.

the lateral off-set for the zero and yaw cases are in different directions. This was not intentional but instead a simple misguided thought during the campaign; it should not influence the discussion of the results.

2.4. CFD methodology

To aid the understanding of the observations made from the tunnel results, CFD simulations were carried out for some of the configurations. Unsteady simulations were conducted using a high-resolution model, the $\kappa - \omega$ SST IDDES with a hexahedral dominated unstructured grid with prism layers on the vehicle surface and the ground. Second order accurate spatial and temporal discretization schemes were used. The computational domain extended 5 vehicle lengths upstream of the first vehicle, 10 vehicle lengths downstream of the last vehicle, 40 vehicle widths wide, and 10 vehicle heights in height. This large size eliminated influences from the domain boundaries on the near vehicle flow. A picture of the computational domain showing the mesh refinement subdomains around the two-truck platoon can be seen in Fig. 6. For the sake of visualization of the vehicles and the near vehicle density boxes, the entire domain is not drawn.

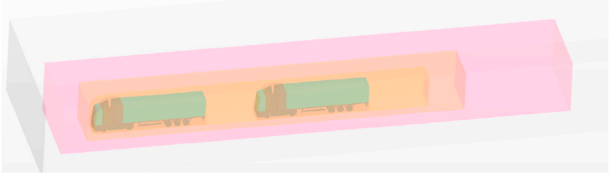

Fig. 6. Part of the computational domain and levels of mesh refinement around the vehicles.

The mesh strategy considered y + as recommended by the turbulence model in all areas where strong gradients were expected. After a mesh study, this resulted in a total mesh size of approximately 220 million cells. The reliability of the numerical method was also tested in terms of appropriate time-step and time-averaging. The time-resolution in the simulations were split up into four sections: three flushing sections and an averaging section. The flushing sections consist of 15 s at a time-step of 0.1s, followed by a 5s period at 0.01s with a final portion of 2s at a time-step of 0.8 ms. The results were then averaged over 10s with a time-step of 0.8 ms. The complete procedure followed the recommendations from Tornell et al. (2020), where the CFD methodology and its validation is described in detail. Notably, a full simulation of all conditions encountered in the wind tunnel tests, including the tunnel geometry, its moving ground system, and the complete set-up to secure the models in place would be prohibitively expensive and time consuming. Instead, an on-road simulation approach was taken with a large domain, a full moving ground, and rotating wheels. This is a common practice in aerodynamic simulations during validation studies and vehicle development, as often the trends observed are acceptable.

3. Results

This section presents the results of this study. First, a Reynolds dependence investigation is conducted and then the results for a single truck are presented. Then, measurements for the leading and trailing trucks are discussed in terms of global drag forces and surface pressures with respect to the varied parameters: inter-vehicle distance, lateral

offset, and yaw. Results from CFD simulations are added to complement the analysis. Finally, the drag of the combined system is examined. All forces have been normalized toward an isolated truck with corresponding wind tunnel conditions. That is, the leading truck forces have been normalized toward a single truck with the distributed suction on, the trailing truck forces toward a single truck with the distributed suction off, and when at yaw conditions they have been normalized toward a single truck in yaw conditions. For the Reynolds sweep study, the forces have been normalized toward the forces at the highest Reynolds number. Throughout the paper, all IVDs and lateral offsets are expressed in full-scale equivalent distances.

3.1. Reynolds number dependence

To validate the results, several Reynolds sweeps were performed during the study (the Reynolds number, Re, is based on the square root of the frontal area). The results are seen in Fig. 7. They show that for a single truck and for a two-truck platoon at zero yaw conditions, the truck's drag practically does not change with an increase in Re. However, when a yaw condition is applied, the system becomes very sensitive to a change in Reynolds numbers below roughly 1.5e6. From 1.7e6 to 1.9e6, almost no change in drag is observed for any cases (0.05–0.8%). Therefore, the following data presented in this paper are for configurations performed at a Re of 1.9e6.

The strong Re dependence of the drag under yaw conditions is most likely caused by a detachment of the flow at the leeward corner of the tractor as indicated by the large change in pressure seen in Fig. 8, a behavior that has also been noted by Cooper (1985). The reason for this behavior being present only under yaw conditions is most likely that the radius of the front corners are close to their critical Re and a small yaw angle therefore causes detachment as the air has to be deflected to a greater degree. This can also be inferred by the time-resolved behavior of a point just behind the leeward radius seen in Fig. 9, where a reduction of higher frequency fluctuations is observed as the Re increases from $1.1*10^6$ to $1.3*10^6$. It is believed that the Re dependent behavior measured in this study is likely due to the sensitive nature of COE trucks when compared to North American style trucks, and potentially due to the addition of ground simulation as shown by Burgin et al. (1986).

3.2. Single truck

The results for a single truck are presented as a reference, Fig. 11. They were obtained with the measurement model with full ground simulation conditions to normalize the drag for the leading truck and with the moving belt on and the distributed suction off to normalize the drag for the trailing truck in the platoon scenario. The drag coefficient at zero yaw was 0.545 and was 0.606 at 5° yaw with full moving ground simulation. Fig. 10 shows the pressure distribution at the base of the truck for zero and 5° yaw. The scale was chosen to allow comparisons with the leading truck in a platoon. As it will be seen later in section 3.3.1, the base pressures for a single truck are lower.

A frequency analysis, illustrated in Fig. 12, reveals that there are two dominant frequencies in the wake that correspond well with the frequencies at the sides of the tractor. These frequencies are believed to be model specific and their cause could not be determined. Frequencies with similar Strouhal numbers can be seen in the drag signal of the CFD simulations as well. They are not believed to be acoustic noise from the main fan of the wind tunnel as that noise is expected to have a significantly higher frequency.

3.3. Two-truck platoon

To map the behavior of the system, forces were measured on the model that was placed on the belt for all configurations. As mentioned, this measurement model functioned as the leading or trailing truck depending on the position of the dummy vehicle.

3.3.1. Leading truck

3.3.1.1. Force measurements. The plots in Fig. 13, show that the trends are similar between a zero yaw and a 5-degree yaw case. At zero yaw, the drag of the leading truck decreases with a decreasing inter-vehicle distance down to 2m, where it then increases slightly as the distance is reduced further to 0.5m. It can also be seen that the largest changes in drag occur between IVDs of 3m–15m. The leading truck is not sensitive to lateral offset when the IVD is greater than 7.5m. However, at shorter distances some sensitivity develops and becomes particularly large at an IVD of 0.5m.

For 5° yaw, the biggest reduction in drag is seen from 3m to 12.5m. The changes in between distances are generally less than those of the zero yaw case, and C_D does not increase as the distance varies from 2m to 0.5m, when no lateral offset is applied. The leading truck is practically unresponsive to lateral offset, except for an IVD of 0.5m where changes are apparent. Due to wind tunnel time limitations, only a few configurations with 1m offset and at low IVDs could be measured, and they all indicate an increase in drag.

To understand this behavior, plots of the surface pressure measured in the tunnel and flow field pictures from numerical simulations are presented next.

3.3.1.2. Pressure measurements and CFD results. For the leading truck, the most significant changes in pressure occur at the base of the trailer.

Fig. 14 shows the average C_p and as expected, it corresponds well with the changes in drag seen in Fig. 13, that is, an increase in the base pressure leads to a decrease in drag, and vice-versa. Furthermore, the

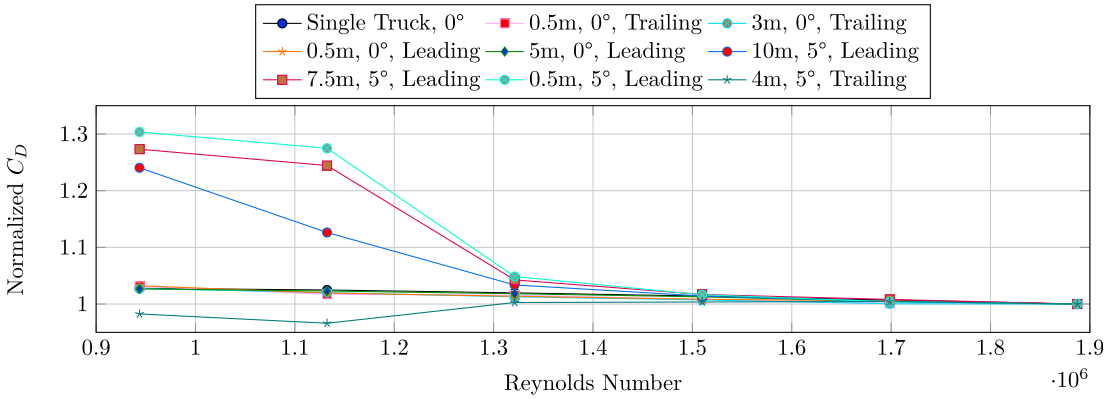

Fig. 7. C_D versus Reynolds number, legend denotes "Inter-vehicle distance, yaw angle, position of truck". Normalized C_D is defined as C_D divided by C_D for the highest velocity of that configuration.

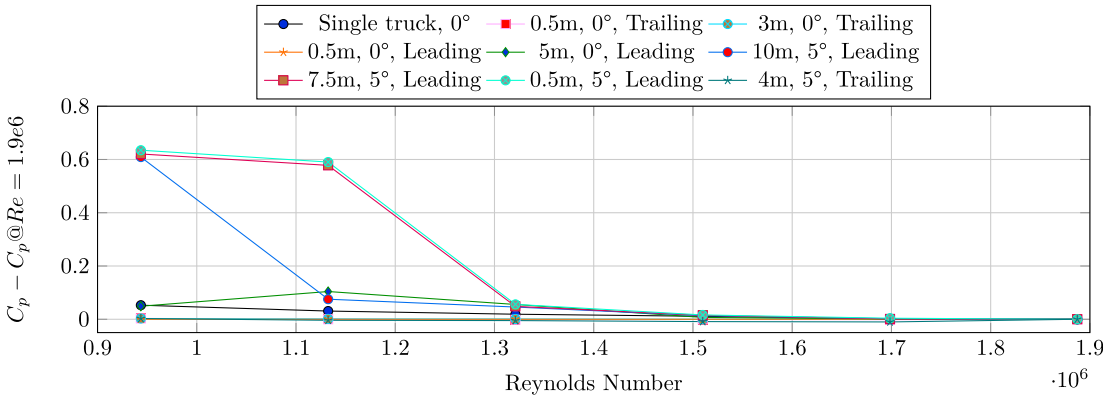

Fig. 8. C_p minus C_p at Re = 1.9*10^6 versus Reynolds number for a point behind the leeward corner of the tractor.

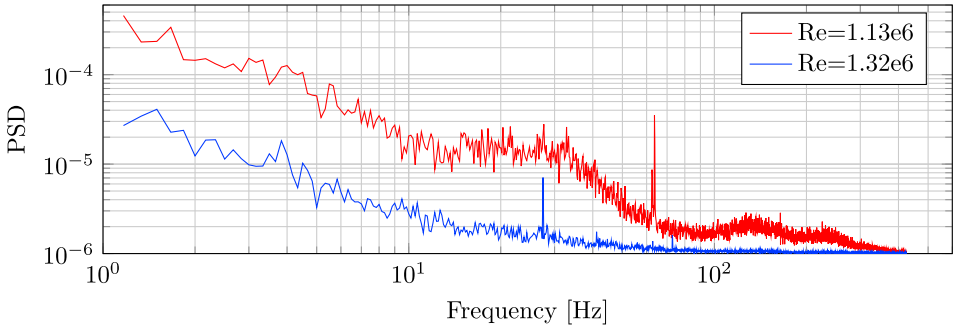

Fig. 9. Frequency spectra at a point behind the leeward corner for the leading truck at a 0.5m IVD and 5° yaw.

Fig. 10. Base C_p distribution for a single truck and full ground simulation conditions.

same behavior can be observed when a lateral offset is applied where a lower base pressure, especially at an IVD of 0.5m, leads to a higher drag. The reason for these changes is a high-pressure region emanated from the stagnation area of the trailing truck. This is apparent in the plots of Fig. 15, obtained from CFD simulations.

From 20m to 10m, the leading vehicle experiences an increase in base pressure due to the closer proximity of the following truck, Fig. 15c and d. The slower improvement in drag at lower IVDs appears to be due to a decreased pressure at the front of the trailing truck, Fig. 15b, thus reducing the effective pressure at the base of the leading vehicle. At very short distances, a change in flow structures occurs, from the two vehicles operating independently, to them operating as a short cavity, similar to a tractor-trailer gap. In such situations, a vortex pair is often formed, lowering the pressure in the gap and thus reducing the base pressure and increasing drag. This is visible in Fig. 16 and confirms what has been shown in previous studies, Allan (1981); Östh and Krajnovic (2012).

Fig. 17 shows the distributed pressure on the base of the leading truck. For the no offset cases, figures a–f, the pressure increases gradually and becomes more uniform as the IVD decreases. The base pressure is generally lower when yaw conditions are present, figures d–f, and there is some asymmetry at high IVDs. For IVDs of 5m and above, the changes are minimal when an offset is applied (for example, Fig. 17b–h and

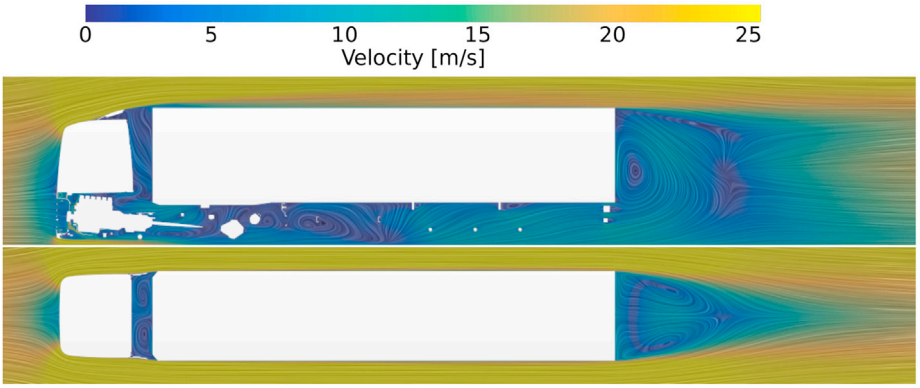

Fig. 11. Velocity magnitude plots obtained with CFD for zero yaw conditions with in-plane streamlines at y = 0 and z = 2.5m from the ground (approximately center of the trailer).

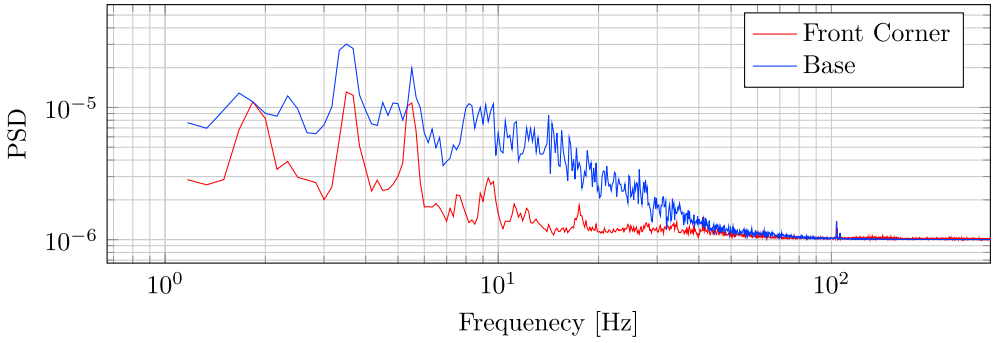

Fig. 12. Frequency spectra at the front corner and base of an isolated truck.

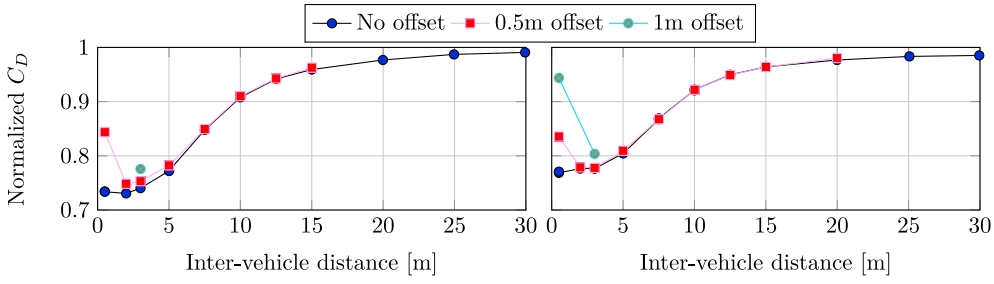

(a) Zero yaw (b) 5 degrees yaw

Fig. 13. Normalized C_D of the leading truck versus inter-vehicle distance with and without lateral offset.

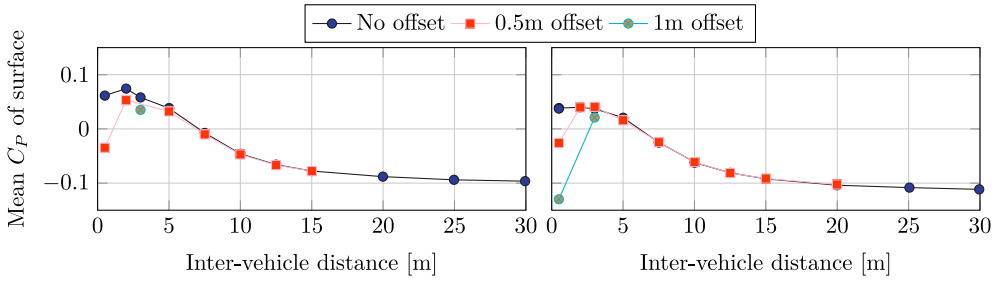

(a) Zero yaw (b) 5 degrees yaw

Fig. 14. Average base C_P for the leading truck versus inter-vehicle distance with and without lateral offset.

Fig. 17f-l). However, for the 0.5m cases, a large change in the base pressure distribution is seen. An area of low pressure appears on one side of the base: right side at zero yaw, Fig. 17g, and left side at 5° yaw, Fig. 17j. This is because the offset direction is different for the yaw and no yaw cases. These results confirm that the main effect of drag reduction for the leading truck is the pressure area emanating from the trailing truck

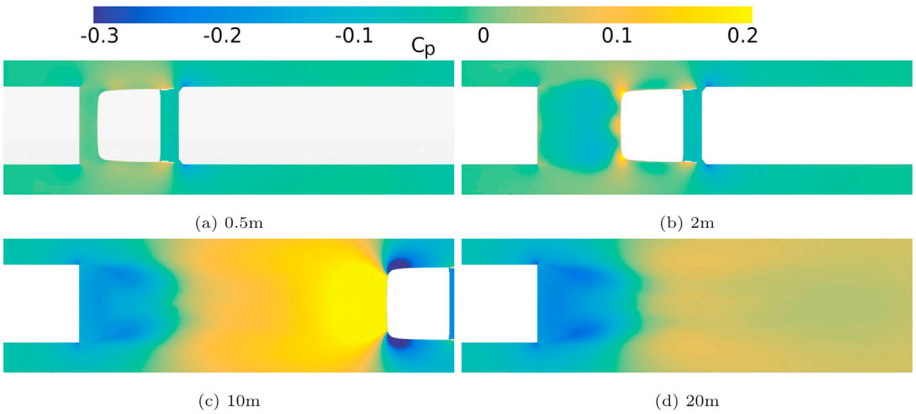

Fig. 15. Time-averaged C_p distribution in between vehicles at z = 2.5m. Results obtained from CFD simulations.

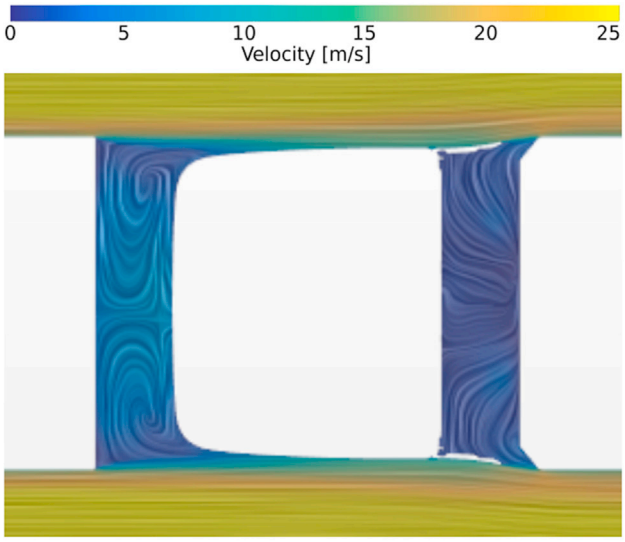

Fig. 16. Velocity magnitude with in-plane streamlines at z = 2.5m for IVD = 0.5m showing the counter rotating vortices in the gap between the vehicles. Results obtained from CFD simulations.

(Fig. 15) creating a higher and more uniform pressure at the base as the IVD decreases. The same phenomenon explains the relative insensitivity to lateral offset: The pressure in front of the stagnation area of the trailing truck is strongly linked to the distance between vehicles, yielding a lower sensitivity to lateral offset at larger IVDs. At very short distances, more effects influence the drag behavior, the lateral offset generates an area similar to a backward-facing step, thus reducing the pressure on the side without the blockage behind it.

Results of the unsteady pressure measurements on the base of the leading truck show the same dominant frequency at various IVDs, shown in Fig. 18. At lower IVDs, however, this frequency becomes less dominant and a broader spectrum is observed. This can indicate that the wake of the leading truck becomes more constrained. A new broad frequency peak is seen for an IVD of 0.5m which could suggest a change in flow behavior; this change in flow behavior can be seen between the vehicles in Fig. 23a-c where the wake changes into a vortex pair.

3.3.2. Trailing truck

3.3.2.1. Force measurements. Fig. 19 shows the normalized drag for the trailing truck. Due to the length of the wind tunnel test section and the limitations in the experimental setup, inter-vehicle distances were limited to a maximum of 5m when measuring forces for the trailing truck. For these short distances, a continuous decrease in drag with decreasing IVD is seen for both yaw cases. At zero yaw, the trailing vehicle is not very sensitive to offset, although a small increase in drag could be measured.

The benefits of platooning for the trailing vehicle are smaller at 5° yaw, as is evident at 5m IVD where the normalized drag is close to unity without offset. Compared to zero yaw, a larger sensitivity to lateral offset is observed. The effect is positive, with the vehicle experiencing less drag. It is to be noted, however that in previous CFD studies by Tornell et al. (2020), an increase in drag for the trailing was calculated as the IVD decreased from 20m to 5m, after which, the same behavior as in the wind tunnel was found. This is similar to the observations of McAuliffe and Ahmadi-Baloutaki (2018, McAuliffe and Ahmadi-Baloutaki, 2019; Salari and Ortega (2018); Lammert et al. (2017) for North American style trucks.

3.3.2.2. Pressure measurements and CFD results. For the trailing truck, the relevant changes in pressure occur around the tractor. Figs. 20 and 21 present, respectively, the mean pressure and the pressure distribution for the various conditions investigated. The values were measured with mean pressure sensors as they were obtained with the dummy model to allow for long IVDs (see Fig. 1). The mean C_p at the front face, Fig. 20a and b, decreases continuously as the IVD decreases for all lateral offsets. This reduction in pressure, confirmed by Figs. 15 and 21, is due to a lower oncoming velocity toward the trailing truck as a result of the wake of the vehicle in front, as shown in Fig. 23. For zero yaw and without a lateral offset, Fig. 21a-c, the pressure at the front face of the truck has a fairly uniform distribution, especially at very low IVDs. When a 0.5m lateral offset is introduced, the pressure becomes less uniform and as the truck moves away from the wake of the leading vehicle, the mean pressure increases slightly, except at an IVD = 0.5m. At yaw conditions the same trend toward a less uniform pressure is seen, however with no apparent increase in the mean C_p curve, Fig. 20b, as in this case, the trailing truck is moved into the wake. This difference between the zero yaw and 5-degree yaw cases is believed to be due to the fact that the trailing truck is moved into the wake in the 5° yaw case and out of the wake in the zero degree yaw case (see Fig. 5).

The surface averaged pressures on the sides and roof, Fig. 20c–g and 20i, show a reversed trend to that of the pressure on the front face. This is expected as a decrease in the oncoming velocity at low IVDs will yield reduced acceleration around these corners. This is confirmed by the CFD results in Fig. 23 for four inter-vehicle distances.

There is, however, a visible difference between the right and left corners of the truck as an offset is applied where the exposed corner, left for zero yaw and right for 5° yaw, experiences a lower pressure. The shielded corners see a slight increase in pressure or no change at greater IVDs, but a reduction at short IVDs. The C_p on the exposed corner does not change significantly as the IVD decreases below 5m for a 0.5m offset.

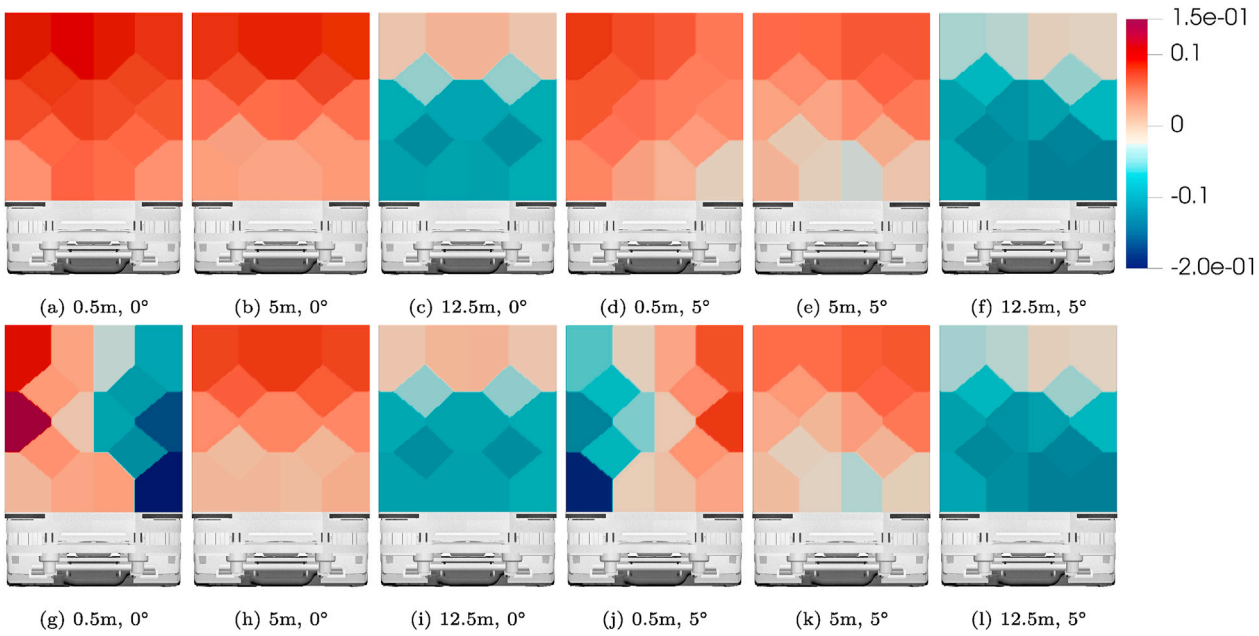

Fig. 17. Base C_P of the leading truck, a-f is with 0m offset and g-l is with 0.5m offset. The values denote "inter-vehicle distance, yaw angle".

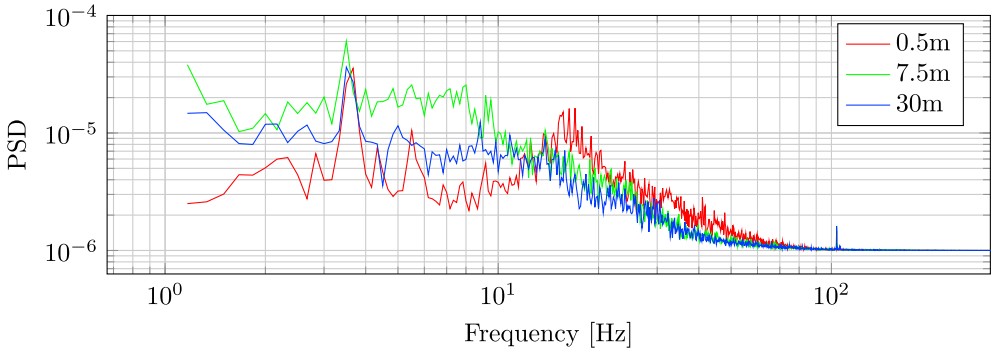

Fig. 18. Frequency spectra at a point on the middle right edge of the base. Leading truck, no offset, zero yaw.

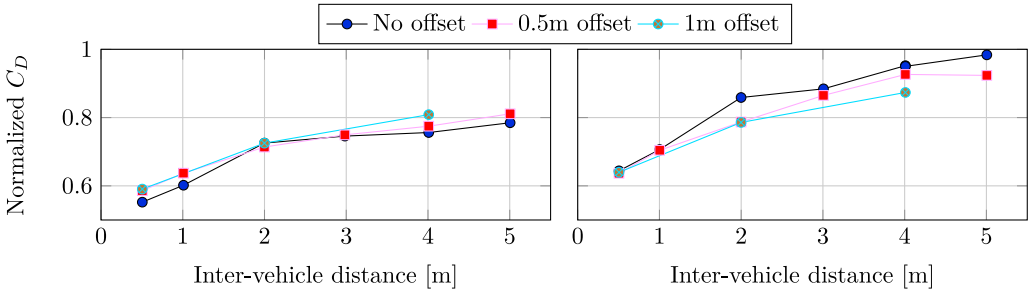

Fig. 19. Normalized C_D of the trailing truck versus inter-vehicle distance with and without lateral offset.

This is in contrast with the behavior when no lateral offset is present. This discrepancy could potentially be explained by a fairly straight shear layer of the wake interacting with the trailing truck forming a stable flow structure at the front as the IVD decreases further.

Looking at the tractor-trailer gap, see Fig. 20h and j, the mean C_p stays nearly constant down to an IVD of 15m where a slight increase is seen as the IVD becomes shorter. This rise in pressure is apparent in Fig. 15 and has been shown in a previous study by Tornell et al. (2020) to increase the drag and be caused by both a lower oncoming flow velocity as well as a change in the flow angle at the front of the truck, thus reducing the efficiency of the roof deflector (Fig. 22). A similar trend is observed for the 5-degree yaw case. In addition, practically no changes are noticeable with an added lateral offset.

All these effects combined produce the changes in drag for the trailing truck where an increase in pressure yields an increase in drag. For IVDs lower than 5m, the variations in drag are dominated by the changes in pressure at the front face of the truck. The decrease in drag with lateral offset at 5° yaw can be explained by the reduction in pressure on the

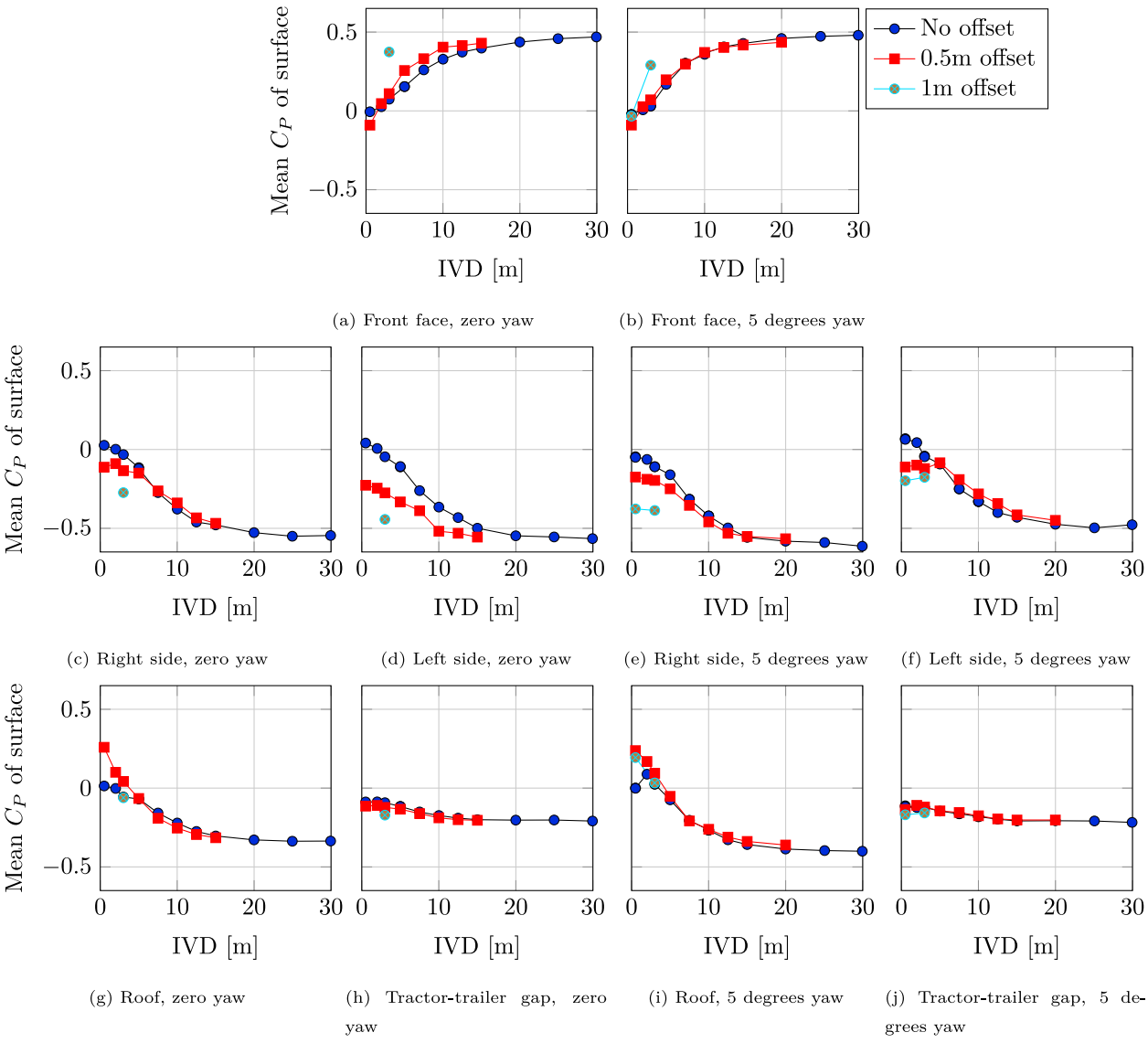

(a) Front face, zero yaw (b) Front face, 5 degrees yaw

(c) Right side, zero yaw (d) Left side, zero yaw (e) Right side, 5 degrees yaw (f) Left side, 5 degrees yaw

(g) Roof, zero yaw (h) Tractor-trailer gap, zero yaw (i) Roof, 5 degrees yaw (j) Tractor-trailer gap, 5 degrees yaw

Fig. 20. Average C_P on the different surfaces on the front of the trailing truck versus IVD with and without lateral offset.

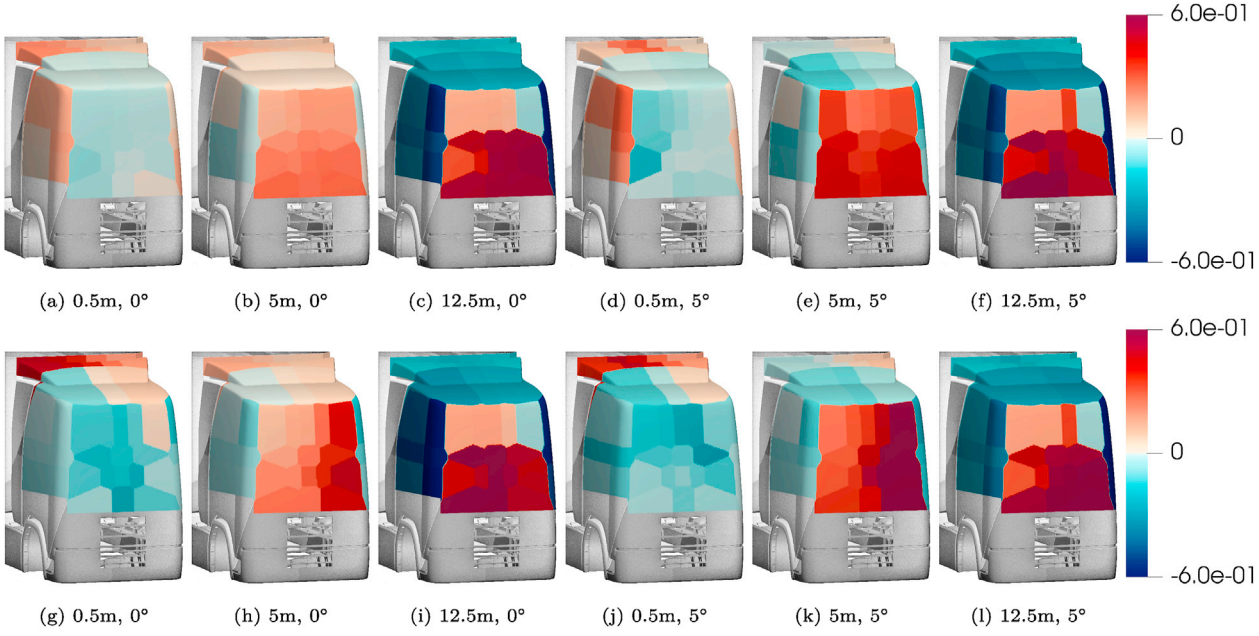

(a) 0.5m, 0° (b) 5m, 0° (c) 12.5m, 0° (d) 0.5m, 5° (e) 5m, 5° (f) 12.5m, 5°

(g) 0.5m, 0° (h) 5m, 0° (i) 12.5m, 0° (j) 0.5m, 5° (k) 5m, 5° (l) 12.5m, 5°

Fig. 21. Tractor C_P of the trailing truck, a-f is with 0m offset and g-l is with 0.5m offset. The values denote "inter-vehicle distance, yaw angle".

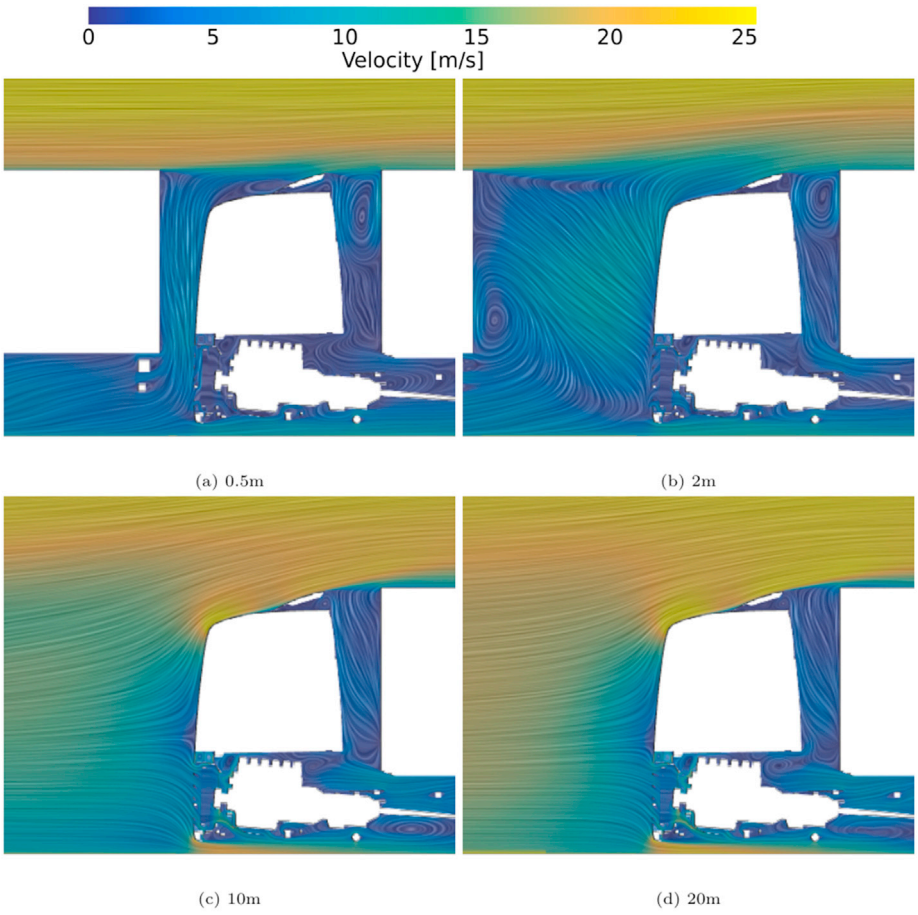

Fig. 22. Time-averaged velocity distribution in between vehicles at centerline. Results obtained from CFD simulations.

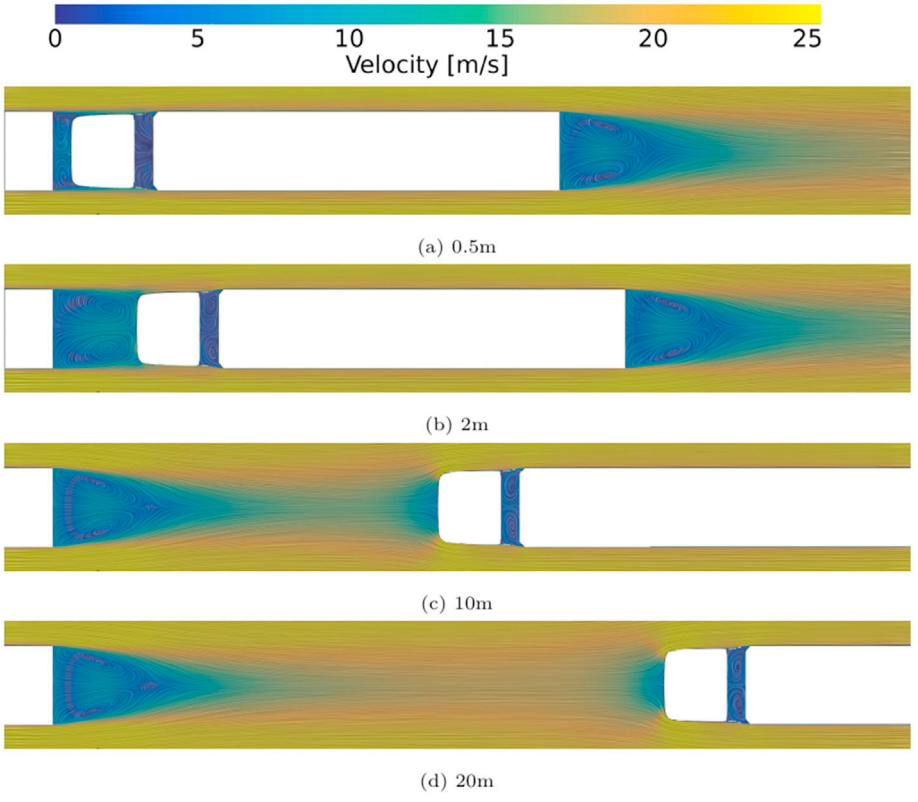

Fig. 23. Oncoming velocity magnitude toward the trailing truck with in-plane streamlines at z = 2.5m. Results obtained from CFD simulations.

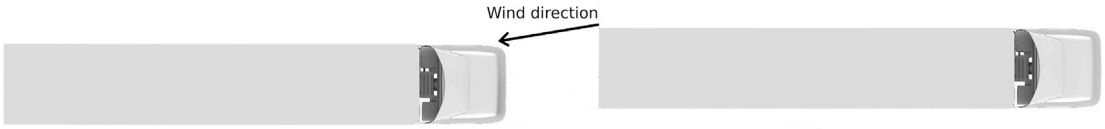

Fig. 24. Intuitively best lateral offset for small yaw angles.

corners and in the tractor-trailer gap, and by the lack of change in pressure at the front face. The opposite is true at zero degrees yaw where an increase in drag is seen with an added lateral offset. For an IVD of 0.5m, this is justified by the large increase in pressure at the roof which compensates for the reduction in pressure at the front face and sides.

As seen, a factor that minimizes drag for the trailing truck under side wind conditions is the lateral offset. It has been shown here that this is not a straightforward task to accomplish as the authors' intuitive expectation would be an offset where the trailing truck front face is in line with the wind from the base of the leading vehicle, see Fig. 24. As with small yaw angles, there is no expectation of large separation at the leeward side and thus the rear wake of the leading vehicle is expected to extend at roughly 5° out from the base of the leading vehicle. This, however, showed not to be the case as the optimal lateral offset is larger than this for the IVDs investigated. This behavior could be explained by the significance of the tractor radii as well as the tractor-trailer gap. Fig. 21k indicates that the offset is too large as the pressure at the front of the truck is very asymmetric. This is however not the case here and a larger lateral offset yields a decrease in drag. Further studies are necessary to understand this behavior.

The unsteady pressures of the trailing truck for an IVD of 0.5m are compared to the results of an isolated vehicle (Fig. 25). These are similar to what was seen on the leading vehicles base, where a decrease in strength of the dominant frequency was observed at the corners and roof of the truck (Fig. 18). This seems to indicate a more constrained flow over the corners which could be explained by the fact that they are in a shear layer of the flow as seen in Fig. 23. Furthermore, differences occur in the tractor-trailer gap, from a few dominant frequencies for an isolated truck to a broad peak at lower IVDs, indicating a change to the flow in this region (Fig. 25b). This could be due to the same effects as the corners and that the pressure fluctuations in the gap are normally driven by the fluctuations at the front radii.

3.4. Combined drag

As different trends in the drag behavior were observed for the leading and trailing truck with a lateral offset, the drag of the two vehicles were combined as a system for the measured range of 0.5m–5m IVD. As can be seen in Fig. 26, at zero yaw, there is a large increase of drag for the system when an offset is applied at an IVD of 0.5m, after which the increase is only minor indicating that the system is not very sensitive to lateral offset when no yaw is present. This is a positive finding as it would give leeway in terms of lateral positioning while still retaining most of the benefits. When yaw conditions are tested, losses are also seen when an offset is applied at an IVD 0.5m; however, for larger IVDs, an improvement in C_D is observed, although relatively small. In yaw conditions, the combined system is more sensitive as experienced by the trailing truck. These results could be of interest when designing systems for vehicle control in platoons. McAuliffe and Ahmadi-Baloutaki (2018) observed similar trends with regard to lateral offset, however with slightly different magnitudes.

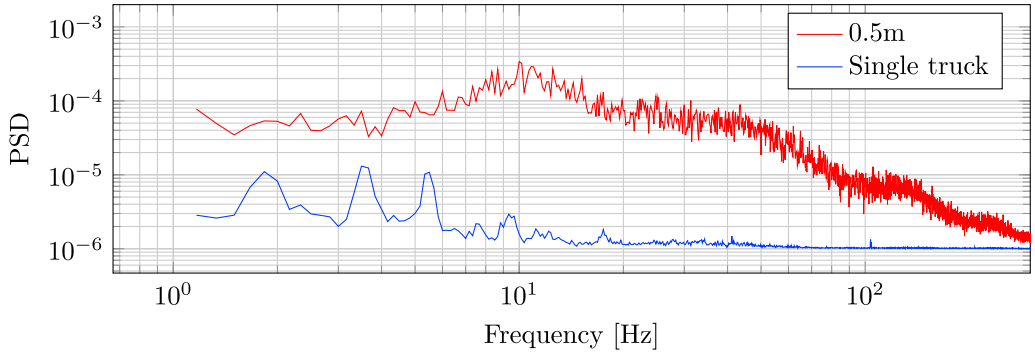

(a) Front corner of tractor

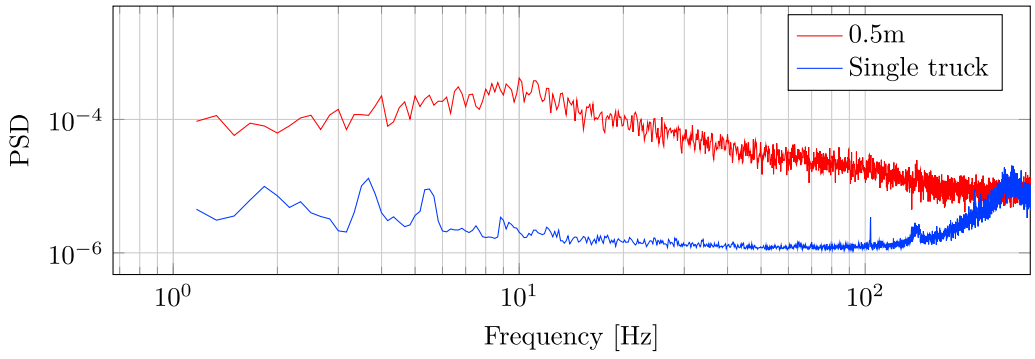

(b) Tractor-trailer gap

Fig. 25. Frequency spectra for the trailing truck.

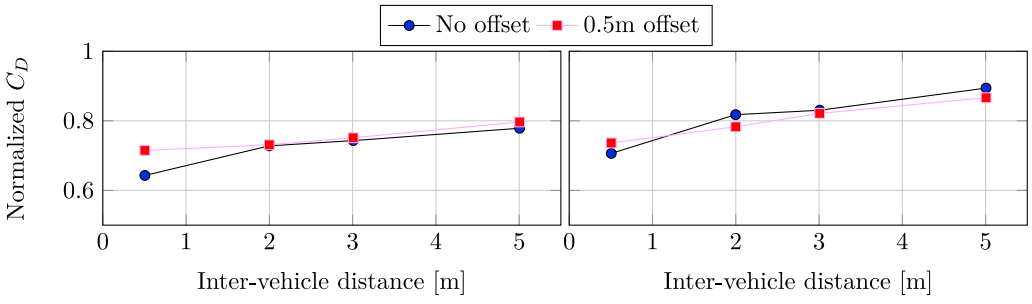

(a) Zero yaw (b) 5 degrees yaw

Fig. 26. Combined drag of the platoon of two trucks. The forces of the two trucks were added and normalized with the sum of the appropriate values for each configuration.

4. Conclusions

In this paper, the aerodynamic behavior of cab over engine (COE) style tractor-trailer combinations in close proximity were studied experimentally in a wind tunnel fitted with a moving ground system. Effects of inter-vehicle distance, lateral offset, and yaw were considered. To enhance the understanding of the flow phenomena, CFD simulations were performed for several of the configurations investigated experimentally. The main observations from this work are the following:

4.1. Leading truck

- For the yaw angles and lateral offset investigated, the drag of the leading truck decreases with a shorter inter-vehicle distance down to 2m, after which an increase is seen. The improvement in drag is due to a higher base pressure caused by the presence of a vehicle behind it. At very low IVDs, a decreased pressure at the front of the trailing truck reduces the effective pressure at the base of the leading vehicle, causing its drag to go up.
- The leading truck is not very sensitive to lateral offset except at very low IVDs. This is because the pressure in front of the stagnation area of the trailing truck is strongly linked to the distance between vehicles, yielding a lower sensitivity to lateral offset at larger IVDs.
- The changes in drag are dominated by the changes in the base pressure.

4.2. Trailing truck

- For the inter-vehicle distances possible to measure in the wind tunnel, the drag of the trailing truck showed a gradual decrease as the IVD changed from 5m to 0.5m. This is because the truck experiences a reduction in stagnation pressure.
- The trailing truck has a complex behavior and is sensitive to the pressure changes on the front face and radii of the tractor as well as the tractor-trailer gap with variations in IVD and lateral offset.
- At low IVDs, an increase in pressure in the tractor-trailer gap, radii, and roof of the tractor which affects drag negatively.

4.3. Combined system

Yaw conditions reduce the efficiency of the platoon. It is important to ensure Reynolds independence when performing measurements in a wind tunnel, especially when studying the system under yaw conditions. The present work has shown that measurements taken at low Re values can yield different drag deltas compared to those taken at a Re number in the Reynolds independent regime. Low sensitivity to lateral offset was observed, with some small drag improvements noticed at yaw conditions.

CRediT authorship contribution statement

Johannes Törnell: Conceptualization, Methodology, Software, Validation, Formal analysis, Investigation, Data curation, Writing – original draft, Visualization. **Simone Sebben:** Conceptualization, Methodology, Resources, Writing – review & editing, Supervision, Project administration, Funding acquisition. **Per Elofsson:** Conceptualization, Methodology, Investigation, Resources, Writing – review & editing, Supervision, Project administration, Funding acquisition.

Declaration of competing interest

The authors declare that they have no known competing financial interests or personal relationships that could have appeared to influence the work reported in this paper.

Acknowledgements

This work has been funded by the Swedish Energy Agency, grant number P44930-1, models were built by Scania CV and the experiments were performed at the Volvo Car Corporation wind tunnel. The simulations were performed on resources provided by the Swedish National Infrastructure for Computing (SNIC) at the National Supercomputing Centre Sweden (NSC) and Chalmers Centre for Computational Science and Engineering (C3SE).

References

●●● Allan, J., 1981. Aerodynamic drag and pressure measurements on a simplified tractor-trailer model. J. Wind Eng. Ind. Aerod. 9 (1), 125–136.
Baker, C., Brockie, N., 1991. Wind tunnel tests to obtain train aerodynamic drag coefficients: Reynolds number and ground simulation effects. J. Wind Eng. Ind. Aerod. 38 (1), 23–28.
Blocken, B., Toparlar, Y., van Druenen, T., Andrianne, T., 2018a. Aerodynamic drag in cycling team time trials. J. Wind Eng. Ind. Aerod. 182, 128–145.
Blocken, B., van Druenen, T., Toparlar, Y., Malizia, F., Mannion, P., Andrianne, T., Marchal, T., Maas, G.-J., Diepens, J., 2018b. Aerodynamic drag in cycling pelotons: new insights by cfd simulation and wind tunnel testing. J. Wind Eng. Ind. Aerod. 179, 319–337.
Burgin, K., Adey, P., Beatham, J., 1986. Wind tunnel tests on road vehicle models using a moving belt simulation of ground effect. J. Wind Eng. Ind. Aerod. 22 (2), 227–236 special Issue 6th Colloquium on Industrial Aerodynamics Vehicle Aerodynamics.
Cooper, K.R., 1985. The effect of front-edge rounding and rear-edge shaping on the aerodynamic drag of bluff vehicles in ground proximity. SAE Trans. 94, 727–757. URL. http://www.jstor.org/stable/44467612.
Ebrahim, H., Dominy, R., 2020. Wake and surface pressure analysis of vehicles in platoon. J. Wind Eng. Ind. Aerod. 201, 104144.
Fletcher, C., Stewart, G., 1986. Bus drag reduction by the trapped vortex concept for a single bus and two buses in tandem. J. Wind Eng. Ind. Aerod. 24 (2), 143–168.
Hackett, J.E., Williams, J.E., Baker, J.B., Wallis, S.B., feb, 1987. On the influence of ground movement and wheel rotation in tests on modern car shapes. In: SAE International Congress and Exposition. SAE International.
Hammache, M., Michaelian, M., Browand, F., mar, 2002. Aerodynamic forces on truck models, including two trucks in tandem. In: SAE 2002 World Congress & Exhibition. SAE International.

Hong, P., Marcu, B., Browand, F., Tucker, A., feb, 1998. Drag forces experienced by two, full-scale vehicles at close spacing. In: International Congress & Exposition. SAE International.

Howell, J., Everitt, K., 1981. The underbody flow of an eds-type advanced ground transport vehicle. J. Wind Eng. Ind. Aerod. 8 (3), 275–294.

J1252, Rev, August 2012. SAE wind tunnel test procedure for trucks and buses. SAE international surface vehicle recommended practice. SAE Standard J1252. URL. https://doi.org/10.4271/J1252_201207.

Jacuzzi, E., Granlund, K., 2019. Passive flow control for drag reduction in vehicle platoons. J. Wind Eng. Ind. Aerod. 189, 104–117.

Lammert, M., Kelly, K., J, Y., 2017. Correlations of Platooning Track Test and Wind Tunnel Data. National Renewable Energy Laboratory.

Le Good, G., Resnick, M., Boardman, P., Clough, B., may 2018. Effects on the aerodynamic characteristics of vehicles in longitudinal proximity due to changes in style. In: CO2 Reduction for Transportation Systems Conference. SAE International.

Le Good, G., Boardman, P., Resnick, M., Clough, B., apr 2019. An investigation of aerodynamic characteristics of three bluff bodies in close longitudinal proximity. In: WCX SAE World Congress Experience. SAE International.

Li, C., Burton, D., Kost, M., Sheridan, J., Thompson, M.C., 2017. Flow topology of a container train wagon subjected to varying local loading configurations. J. Wind Eng. Ind. Aerod. 169, 12–29.

Ljungskog, E., 2019. Evaluation and Modeling of the Flow in a Slotted Wall Wind Tunnel. Doctoral thesis. Chalmers University.

Maleki, S., Burton, D., Thompson, M.C., 2019. Flow structure between freight train containers with implications for aerodynamic drag. J. Wind Eng. Ind. Aerod. 188, 194–206.

Marcu, B., Browand, F., mar, 1999. Aerodynamic forces experienced by a 3-vehicle platoon in a crosswind. In: International Congress & Exposition. SAE International.

McAuliffe, B.R., Ahmadi-Baloutaki, M., 2019 apr. An investigation of the influence of close-proximity traffic on the aerodynamic drag experienced by tractor-trailer combinations. SAE.Int. J. Adv. Curr. Pract.Mobil., 2019-01-0648

McAuliffe, B.R., Ahmadi-Baloutaki, M., jun 2018. A wind-tunnel investigation of the influence of separation distance, lateral stagger, and trailer configuration on the drag-reduction potential of a two-truck platoon. SAE. Int. J.Commerc.Veh 11, 125–150.

Östh, J., Krajnovic, S., 2012. The flow around a simplified tractor-trailer model studied by large eddy simulation. J. Wind Eng. Ind. Aerod. 102, 36–47.

Salari, K., Ortega, J., apr 2018. Experimental investigation of the aerodynamic benefits of truck platooning. In: WCX World Congress Experience. SAE International.

Sardou, M., 1986. “Reynolds effect” and “moving ground effect” tested in a quarter scale wind tunnel over a high speed moving belt. J. Wind Eng. Ind. Aerod. 22 (2), 245–270 special Issue 6th Colloquium on Industrial Aerodynamics Vehicle Aerodynamics.

Schito, P., Braghin, F., apr 2012. Numerical and experimental investigation on vehicles in platoon. SAE. Int. J.Commerc.Veh 5, 63–71.

Söderblom, D., 2012. Wheel Housing Aerodynamics of Heavy Trucks. Doctoral thesis. Chalmers University.

Söderblom, D., Elofsson, P., Hjelm, L., Lofdahl, L., apr 2012. Experimental and numerical investigation of wheel housing aerodynamics on heavy trucks. SAE. Int. J.Commerc.Veh, 2012-01-0106.

Sternéus, J., Walker, T., Bender, T., apr 2007. Upgrade of the volvo cars aerodynamic wind tunnel. In: SAE World Congress & Exhibition. SAE International.

Tornell, J., Sebben, S., D, S., 2020. Influence of inter-vehicle distance on the aerodynamics of a two-truck platoon. Int. J. Automot. Technol. (Accepted for publication.

Tsuei, L., Savaş, Ömer, 2001. Transient aerodynamics of vehicle platoons during in-line oscillations. J. Wind Eng. Ind. Aerod. 89 (13), 1085–1111.

Watkins, S., Vino, G., 2008. The effect of vehicle spacing on the aerodynamics of a representative car shape. J. Wind Eng. Ind. Aerod. 96 (6), 1232–1239, 5th International Colloquium on Bluff Body Aerodynamics and Applications.

Yamashita, T., Makihara, T., Saito, Y., Kato, C., Takayama, R., Takayama, T., Yamade, Y., apr 2018. Effects of Moving Ground and Rotating Wheels on Aerodynamic Drag of a Two-Box Vehicle.